Supporting Information for the article: "Measurement of the curvature-dependent surface tension in nucleating colloidal liquids"

Methods

We use a two-component solvent of 3-Methyl Pyridine (3MP) and heavy water [1] with mass fractions of 0.28 and 0.72, respectively. This solvent separates into 3MP-rich and water-rich phases upon increasing the temperature above $T_c = 39.5$ °C, the solvent critical point. In the homogeneous solvent at room temperature, we suspend Poly-n-isopropyl acrylamide (PNIPAM) particles at a weight fraction of $\sim 0.3\%$, in which they are closely refractive-index and density-matched with the solvent, making the suspension transparent, and preventing particle sedimentation. The particles are labelled with a fluorescent dye that makes them visible as bright spots under fluorescent imaging. The PNIPAM particles undergo a reversible change in size below the studied temperature regime, saturating to a constant size for temperatures $T \geq 38$ °C as shown in Fig. 1. Thus, in the temperature regime studied, the particle size is constant, and only the particle interaction changes due to critical Casimir forces. The particle radius is $r_0 = 250$ nm with a polydispersity of 3%. The effective particle volume fraction of the final suspension is 2%.

Close to the phase separation temperature T_c of the binary solvent, solvent fluctuations increase and become long-range, and their confinement between particle surfaces at close distance give rise to critical Casimir forces between the particles. Because these solvent fluctuations depend in a well-known universal manner on temperature, temperature provides a unique control parameter to tune the particle interaction. The Critical Casimir force thus provides effective particle interactions that may be regarded similar to those of molecular liquids, with range and strength controlled by temperature.

A specially designed heating set-up allows us to control the temperature of the suspension with a stability of $\pm$ 0.01 °C while imaging the individual particles with confocal microscopy. To induce critical Casimir attractions between the particles, we heat the suspension to some temperature ΔT below T_c. We observe the nucleation of the colloidal liquid by varying critical Casimir interactions continuously in a temperature range between 0.5 and 0.2 °C below T_c. In this temperature range, the particle

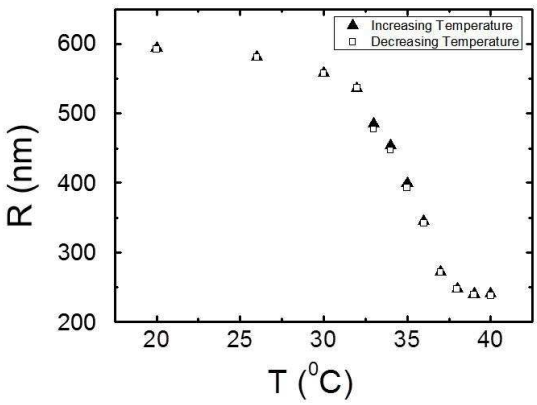

FIG. 1. Particle size as a function of temperature measured by dynamic light scattering on a dilute suspension.

size is independent of temperature as determined by dynamic light scattering. Furthermore, the solvent correlation length is $\sim$ 30 to 40 nm, only a small fraction of the particle size so that many-body effects are still limited. The direct temperature control of particle interactions allows us to drive the colloidal system reversibly through the gas-liquid transition, and to follow the liquid nucleation and process directly at the particle scale, as shown by supplementary movies S1 and S2. We note that the system is very stable, and can be driven many times through the gas-liquid phase transition without any signs of irreversibility (e.g. particle aggregation).

Confocal microscope imaging of the colloidal droplets

We use a fast confocal microscope (Zeiss 5 Live), and a 100x immersion-oil objective with a numerical aperture of 1.4 to image the individual particles. Despite their small size, the particles can be easily resolved in the liquid phase due to the relatively low particle volume fraction in the liquid, which is merely $\phi \sim 20\%$; as a result the imaged intensity distributions of the individual particles can be clearly distinguished, and the particles well resolved in space. During image acquisition, the particles diffuse in space. The mean-square displacement of liquid particles is roughly an order of magnitude smaller than that of isolated (gas-like) particles on the time scale of $\sim$10 sec, see Fig. 2. This means that during the entire acquisition time of a confocal stack of 20 seconds, a liquid particle diffuses roughly 2.5 microns, which is a few times its own diameter. During the time needed to scan a vertical distance corresponding to the interparticle distance (500 nm), liquid particles exhibit a mean-square displacement

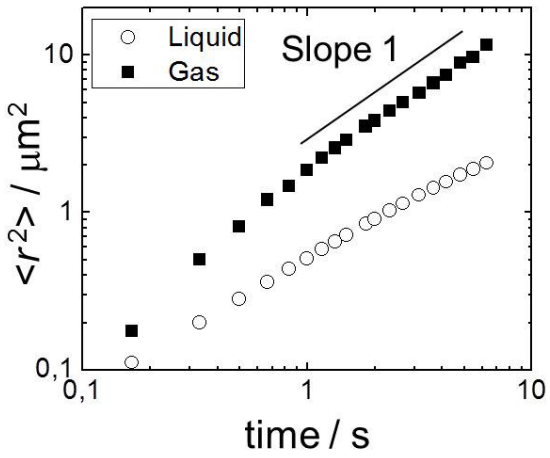

FIG. 2. Mean-square displacement of particles in the liquid and gas phase as a function of time. Particles in the liquid are diffusive, but their mean-square displacement magnitude is smaller by a factor of 10 than that of the gas particles due to crowding effects.

roughly a factor of three smaller than gas particles, diffusing a distance of the order of their radius. This means that the entire three-dimensional scan represents a cut through space-time (i.e. includes some time evolution also); however, the effect at the interparticle scale is limited as can be seen from the pair correlation function, clearly sharpening with increasing supersaturation as expected for a cooled liquid, as shown in Fig 4c of the main manuscript. From the images, particle centers are located in three dimensions using recent extensions of the original code by Crocker and Grier [2]. Due to the relatively low particle volume fraction ($\phi \sim 20\%$), the particles can be distinguished and localized in space easily, despite their relatively small size.

Ellipsoidal fitting

To measure the surface tension of nuclei, we fitted them (identified as connected clusters of highly coordinated particles) by ellipsoids. Reconstructions of typical colloidal liquid nuclei are shown in Fig. 3 together with their ellipsoidal fits. We compare fits by a general ellipsoid (with independent radii a,b,c) with fits by an ellipsoid of revolution (with radii a=b and c). We find that the surface areas of best-fit general ellipsoids and best-fit ellipsoids of revolution are very similar, differing by a few per mill only, much below the experimental error margin, as shown in Table 1. We therefore conclude that the results are robust with respect to the type of ellipsoid used for fitting. In the main paper, we used general ellipsoids for fitting, as the extra

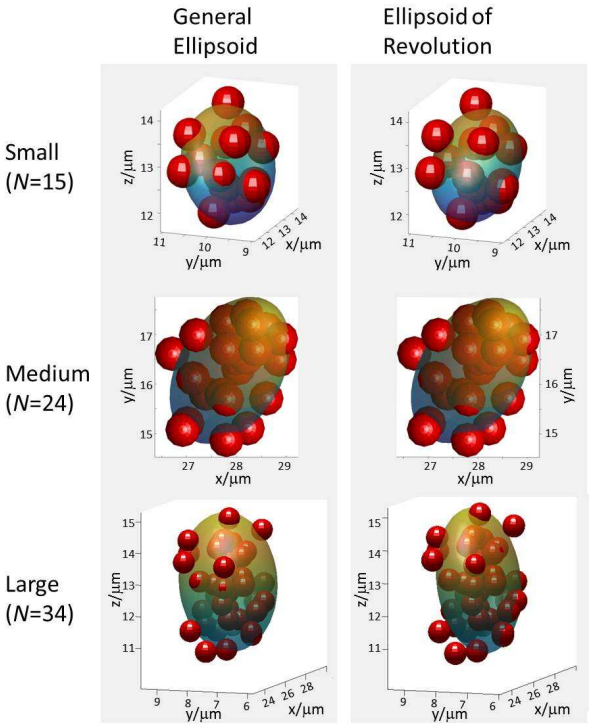

FIG. 3. Reconstructions of nuclei and their ellipsoidal fit. The reconstructions show typical examples of small, medium, and large nuclei, fitted by general ellipsoids, and ellipsoids of revolution. We find that the difference in surface area of the general ellipsoid versus the ellipsoid of revolution is negligible, as shown in Table 1. Thus, our results are robust with respect to the type of ellipsoid used for fitting.

parameter provides additional freedom to adequately describe the nucleus shape, but the difference to other ellipsoids is negligible.

Comparison of second-order correction with computer simulation results

Our colloidal gas-liquid equilibrium follows the universal scaling prediction of molecular liquids [3]. Like molecular liquids, our colloidal system exhibits a critical point for a particle density ρ_c^{liq} and temperature T_c^{liq}, where the gas-liquid equilibrium vanishes. This allows us to compare with computer simulations by normalization: the normalized density $\rho/\rho_c^{\mathrm{liq}}$ as a function of normalized temperature T/T_c^{liq} follows the universal prediction known to apply to many molecular liquids [3].

To compare the specific value of the second order correction, κ, to values obtained in simulations, we determine, from the measured pair potential, the reduced temperature of our system. We determine that the attractive strength of the particles at

Nucleus	$A_{\mathrm{gen}}/\mu m^3$	$A_{\mathrm{rev}}/\mu m^3$	rel. diff.
Small (N=15)	14.494	14.453	0.2%
Medium (N=24)	31.790	31.785	0.031%
Large (N=34)	39.271	39.207	0.16%

TABLE I. Surface areas of ellipsoidal fits to small, medium and large nuclei, for fitted general ellipsoid A_{gen}, and ellipsoid of revolution A_{rev}, and relative difference, $(A_{\mathrm{gen}} - A_{\mathrm{rev}})/A_{\mathrm{gen}}$.

the experimental temperature $T \simeq 39$ °C corresponds to a reduced temperature of $T/T_{\mathrm{c}}^{\mathrm{liq}} = 0.72$ [3]. Computer simulations report values of $\kappa = 1.35\ k_{\mathrm{B}}T$ and $\kappa = 2\ k_{\mathrm{B}}T$ for reduced temperatures of 0.78 and 0.68 T_{c} [4], respectively. Our measured value of $\kappa = 1.35\ k_{\mathrm{B}}T$ falls within this range, and therefore agrees well with these simulation values.

Mean field estimate of second order correction

In the manuscript, we show that the simple mean-field expression eq. (1) allows a surprisingly accurate estimate of the surface tension based on the pair potential $U(r)$ and pair correlation function $g(r)$ of the liquid structure. Similar to equation (1), we can also estimate the bending rigidity directly from the pair potential and pair correlation function using [5,6].

$$\kappa = \frac{\pi\,\rho^2}{144}\int_0^\infty dr\ r^6\,U'(r)g(r)\,.$$

Here, we have, similar to the derivation of eq. 1, assumed that the gas is infinitely dilute and homogeneous up to the dividing interface. Using the experimentally measured $g(r)$ and $U(r)$, we obtain $\kappa = 1.3\ k_{\mathrm{B}}T$, in very good agreement with the value $\kappa = 1.35\ k_{\mathrm{B}}T$ resulting from the fit in Fig. 4b.

References:

1. D. Bonn, J. Otwinowski, S. Sacanna, H. Guo, G. Wegdam and P. Schall, Phys. Rev. Lett. **103**, 156101 (2009).

2. See http://tacaswell.github.io/tracking/html/, Maria Kilfoil's code.

3. V.D. Nguyen, S. Faber, Z. Hu, G.H. Wegdam and P. Schall, Nature Comm. **4**, 1584 (2013).

4. B.J. Block, S.K. Das, M. Oettel, P. Virnau and K. Binder, J. Chem. Phys. **133**,

154702 (2010).

5. E.M. Blokhuis and D. Bedeaux, Physica A **184**, 42 (1992).

6. M. Napiorkowski and S. Dietrich, Phys. Rev. E **47**, 1836 (1993).